Results in Nonlinear Analysis 7 (2024) No. 4, 84–92
https://doi.org/10.31838/rna/2024.07.04.011
Available online at www.nonlinear-analysis.com

Results in Nonlinear Analysis
ISSN 2636-7556

Peer Reviewed Scientific Journal

Mathematical modelling for joining carbon nanostructures: fullerene and torus

Nawa A. Alshammari

Department of Mathematics, Saudi electronic University, Riyadh, Saudi Arabia.

Different configurations of carbon nanostructures, including carbon nanotori and carbon fullerenes, have been identified using experimental techniques. These structures are used at the nanoscale in many different fields, and their inclusion may lead to novel combinations with improved features and applications. In this study, a carbon fullerene and nanotorus combination was identified. Two different approaches that depend on energy minimization were used to predict the conjoining curves. The primary model targets the reduction of elastic energy focusing on axial curvature alone, but the alternative model incorporates the Willmore energy, that accounts both the rotational and the axial curvatures. Due to the catenoid status as an optimal minimiser of this energy, a segment of it employed to facilitate the fusion of two nanostructures. Our findings reveal that both proposed models successfully identify the junction area among nanostructures, allowing for the creation of integrated nanostructures through either method.

Key words and phrases: Carbon fullerene carbon nanotube elastic energy calculus of variations

Mathematics Subject Classification (2010): 35F21, 35F99, 49L99.

1. Introduction

Nanotechnology is a popular subject of study in many fields owing to its wide range of practical applications. Different forms of carbon nanostructures have diverse potential applications in many nanoscale devices because of their unique properties [3–5]. The ability to combine carbon nanostructures has attracted considerable attention owing to the integrated forms having enhanced properties [6]. Interestingly, the literature contains new uses of integrated nanostructures such as energy storage, drug delivery, and scanning tunnelling microscopy [9].

Email address: N.Alshammari@seu.edu.sa (Nawa A. Alshammari)

Received June 6, 2024; Accepted October 10, 2024; Online October 25, 2024

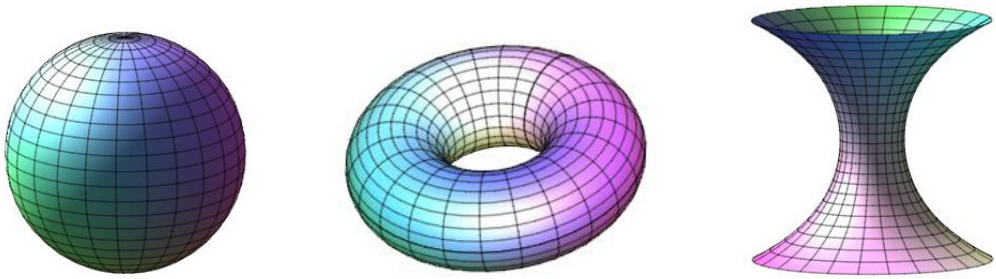

(A) Spherical surface (B) Torus surface (C) Catenoid surface

Figure 1: Structure of surfaces.

Carbon fullerene $C60$, also known as buckminsterfullerene or buckyballs, was discovered in 1985 [10]. It has a hollow cage structure with 60 vertices enclosing a spherical carbon atom, as shown in Fig. 1A. These nanostructures have several distinctive and specific properties that hold promise for a variety of applications, including antioxidants, treatments for neurodegenerative disorders [11], transistors, electron-spin quantum computers [12], electron acceptors, photovoltaics [14], molecular diodes or rectifiers [13] and biosensors [15].

Carbon nanotori or nanorings are formed by connecting the two ends of carbon nanotubes (Fig. 1B). The structures of these compounds have been investigated in numerous studies for their electronic and magnetic properties [16–19]. They can generate gigahertz frequencies because of their circular shape and special resonance characteristics, they have the ability to produce gigahertz frequencies, which makes them attractive candidates for use in high-frequency oscillators and signal processing equipment. In addition, they are employed in ultrafast optical filters and nanoantennae that are sensitive to high-frequency electromagnetic signals [20]. In addition, they have potential for application in terahertz communication systems [16].

Accordingly, different methods have been used to model scenarios for conjoined nanostructures. Previous studies used the elastic energy method to combine various nanostructures. This approach states minimizing a curvature-dependent energy function to obtain the optimal joining surfaces between the two nanostructures. This gives rise to derive the Euler-Lagrange equation for extremal curves or surfaces that minimize this energy that joins the two different nanostructures. Many studies have modelled the conjoining of nanostructures based on this model; e.g., The combination of several carbon nanomaterials, such as tubes-fullerenes, graphenes-fullerenes, cones-fullerenes, graphenes-tubes, fullerenes-fullerenes, cones-cones [21, 23]. Furthermore, this model has been used to form boron nitride nanostructures [24, 25] . Predicting the geometries of the two conjoining nanostructures, we employed the Willmore energy function from our previous study [8]. In order to find the joining surfaces in the three-dimensional structures between nanostructures, this model takes into account each of the axial and rotational curvatures. Correspondingly, due to their status as perfect minimisers of the Willmore energy, catenoids are employed to connect the nanostructures, as shown in Fig. 1C. Additionally, this model indicates the conjunction of a carbon nanotube with a fullerene, two fullerenes, and carbon nanotubes with a carbon nanotorus [8][26]. In addition, this model combines different boron nitride nanostructures [22]. Typically, Willmore energy is utilised to simulate surface bending that occurs with the stretching of the membranes of cells [27], spinal vertebrae segmentation [28], and red blood cell activity [29]. Furthermore, other structures of boron nitride can be examined by using the presented approach, such as helical graphite [32], atypical helices [31], nanoneedles, helical hexagons [30], horizontally elongated spirals [33] and cylindrical structures [34].

Although previous studies have considered different conjoining nanostructures, the conjunction between carbon and fullerenes has not been studied. Therefore, this study's objective was to model the conjoining curve between the nanostructures by using both models.; first: the elastic energy model in 2D, and second, the Willmore energy model in 3D.

In this case of joining, we have a continuous donut-shaped surface with varying curvature among the inner and outer radii. The transition tends from the smooth to the polyhedral of the fullerene. The differences between surface energy and curvature among the structures must be considered. The model was adapted to ensure that the transition does not introduce excessive strain or distortions, but this adaptation is implicit in the application of the existing framework. In contrast with joining two fullerenes, we have structures of two polyhedral with same curvatures. The main target in the transition is to maintain the symmetry and structural integrity of the carbon atoms configuration. In addition, the energy minimizes the bending and stretching energy with united framework of carbon atom.

Furthermore, the joined structures are $C1$-smooth across the joins. That is the gradients are continuous at the junctions. This includes a smooth transition in the tangent direction without any abrupt changes in slope. Whereas if there is a jump in the second derivatives, it shows that the curvature is not continuous. This jump means that while the structures are smooth in terms of slope, they may not have a smooth curvature ($C2$ continuity). Moreover, in some situations a jump in the second derivatives influences the accuracy of the model as in applications requiring precise control over stress distributions or where smooth curvature is critical. Further, $C1$ continuity can be sufficient in many practical applications, mainly those focused on overall shape and structural stability. The main target in these situations is ensuring that the structure is smooth and free of sharp edges, which is achieved with $C1$ continuity.

Moreover, if we compare the joining of a fullerene and a nanotorus with the joining of fullerenes of two different sizes, both scenarios use same profile curve to include a smooth transition ($C1$ continuity) between the joined structures. However, because every structure has a different curvature and topographical characteristics, there are variations in the geometry problems between the two scenarios. In particular, The toroidal curvature makes the joining between nanotorus and fullerene more complex than the joining between two fullerenes of different sizes. In addition, the topographical nature of the nanotorus raises additional considerations to the energy minimization model to ensure smooth transitions and structural stability.

The basic formulas that depict the region of interconnection between nanostructures are introduced in the next section. The results are presented in Section 3. The paper is concluded in Section 4.

2. Models

2.1. Primary approach

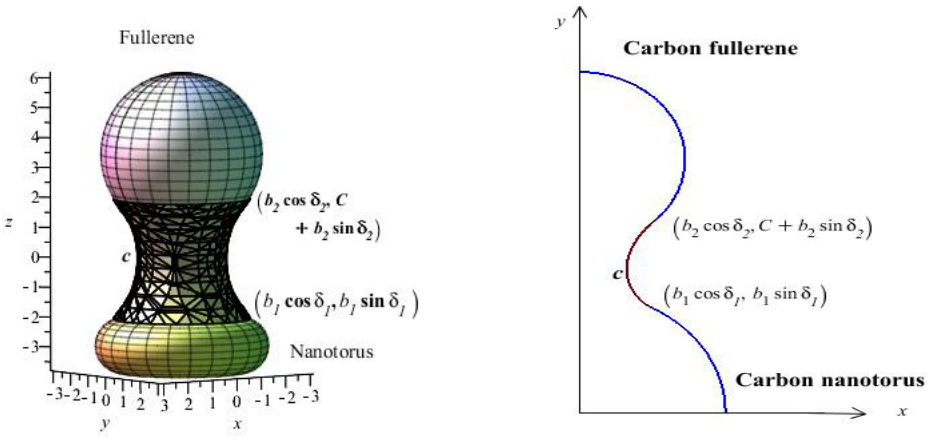

(A) 3D configuration (B) 2D configuration

Figure 2: Geometry of the primary approach's conjunction.

This subsection investigates the application of the calculus of variation for identifying the curve that connects nanostructures of carbon. Specifically, we make the assumption that a torus at the nanoscale exhibits symmetry around the *z*-axis, having its minor radius *a* along with main radius *R* positioned at the centre. In contrast, the fullerene is positioned in such a way that its axis is aligned with the *y*-axis and has a radius of b. The beginning distance above the *xz*-plane, denoted as y_0, is unknown. Furthermore, *C*, which may be obtained in the solution, is the space in the *y*-direction between the two forms. If both nanostructures exhibit rotational symmetry around the *y*-axis, the position y_0 will lie on a 2-dimensional *xy* plane.

The curve links the structures located at the coordinates $(b_1\cos\delta_1, b_1\sin\delta_1)$ and $(b_2\cos\delta_2, C+b_2\sin\delta_2)$ with the torus and the fullerene, respectively, spanning a precise arc length of *c*. as illustrated in Fig. 2.

Utilising the identical computations as presented in the reference [35], where $y=y(x)$ represents an element of arc length *ds*, the sought-after curve that minimises $J_1[y]$ is of the given form

$$J_1[y]=\int_0^c \kappa_1^2 ds+\lambda\int_0^c ds,$$

Here, κ_1 represents the axial curvature and λ is a Lagrange multiplier associated with the fixed length constraint. Because the model only takes into account the profile curve in this particular slice, the rotational curvature κ_2 does not exist in this planar slice across the junction. But κ_2 is in fact greater than zero when the complete rotationally symmetric surface is taken into account. Also *c* is the given length of the curve. By applying the variational principle to minimize $J_1[y]$, we find Equation (1) represents the Euler-Lagrange equation associated with the extremals of the functional $J_1[y]$,

$$\kappa_1=\pm\left(\lambda+\frac{\alpha}{(1+y'^2)^{\frac{1}{2}}}\right)^{\frac{1}{2}}, \tag{1}$$

2.2. Alternative approach

This subsection outlines the application of the Willmore energy function (WEF) to determine the surface where carbon forms in nanoscale are connected. (WEF) J_2 is realize as the integral over the joining surface of the mean curvature squared. Namely, the mean curvature H is identified by the sum of the axial curvature κ_1 and the rotational curvature κ_2 $(i.e., H=\kappa_1+\kappa_2)$. In addition, J_1 covers a length restriction and J_2 contains an area restriction, representing the two-dimensional analogue,

$$J_2[y]=\int(\kappa_1+\kappa_2)^2 d\mu+\lambda\int d\mu,$$

where, $d\mu$ refers to the element of the area, *H* represents the mean curvature and λ indicates a Lagrange multiplier associated with an area restrictions. Because the axial curvature κ_1 and the rotational curvature κ_2 are balanced, a catenoid is a minimum surface, meaning that its mean curvature $H=\kappa_1+\kappa_2$ equals zero. It is therefore an absolute minimizer of the Willmore functional without constraints [7]. This scenario is modified though, when an area limit is added. It will be necessary to carefully take into account the outside radii of both structures in order to link a fullerene and a torus smoothly utilizing a catenoid. These radii need to meet specific requirements in order for the join to be sufficiently smooth, which we describe in the analysis that follows.

Given that catenoids are the most optimal solutions in terms of minimising Willmore energy, we made the assumption that the connection would possess a catenoid surface with coordinates as:

$$x=a\cos\theta,\ y=a\sin\theta,\ z=f(a),$$

referring to Fig. 1C.

Furthermore, the mean curvature can be expressed as

$$H=\kappa_1+\kappa_2=-\frac{f''(a)}{(1+f'^2(a))^{\frac{3}{2}}}-\frac{f'(a)}{a\sqrt{f'^2(a)+1}},$$

if this is equal to zero, it results in an absolute minimiser of the Willmore energy, and the solution is obtained as the following:

$$f(a) = \pm \frac{\ln\left(c_1 a + \sqrt{c_1^2 a^2 - 1}\right)}{c_1} + c_2,$$

with constants of c_1 and c_2. Additionally, the solution can be written as:

$$f(a) = \pm \frac{\cosh^{-1}(c_1 a)}{c_1} + c_2. \tag{2}$$

This suggests that the connecting surface functions as a catenoid, forming the link among the two nanostructures of carbon. For further information, refer to the reference [8].

3. Results

3.1. Results via the primary approach

In this instance, the elastic energy was utilised to establish the connecting curve amongst carbon forms. Here, the value of y' varies from $x = b_1 \cos\delta_1$ to $x = b_2 \cos\delta_2$ as $-\cot\delta_1$ to $-\cot\delta_2$. Therefore, the boundary condition (B. C.) may be expressed as $y'(b_2 \cos\delta_2) = -\cot\delta_2$. Since the joint curvature in this situation continues to be positive over the whole arc length c, then the positive value of equation (1) is taken into account. Using $\tan\theta = y'$ in (1) yields

$$\kappa_1 = (\lambda + \alpha\cos\theta)^{1/2}.$$

By defining the curvature as $\kappa_1 = \frac{y''}{(1+y'^2)^{3/2}}$ and considering the derivative of y, we can derive

$$\frac{dy}{d\theta} = \frac{\sin\theta}{(\lambda + \alpha\cos\theta)^{1/2}},$$

and

$$\frac{dx}{d\theta} = \frac{\cos\theta}{(\lambda + \alpha\cos\theta)^{1/2}}.$$

Given the B.C. at the position $(b_1\cos\delta_1, b_1\sin\delta_1)$, we may conclude that

$$y(\phi) = 2\beta k(\cos\phi_1 - \cos\phi) + b_1 \sin\delta_1,$$

where δ_1 represents the first angle of connection with the torus, and ϕ_1 is defined as $\phi_1 = \sin^{-1}\left(\sqrt{\frac{1-\sin\delta_1}{2k^2}}\right)$.

In contrast, if we use the B.C. at points $(b_2\cos\delta_2, C + b_2\sin\delta_2)$ and $\phi_2 = \sin^{-1}\left(\sqrt{\frac{1-\sin\delta_2}{2k^2}}\right)$ we obtain

$$C = 2\beta k(\cos\phi_1 - \cos\phi_2) + b_1\sin\delta_1 - b_2\sin\delta_2, \tag{3}$$

where $\theta \in [\psi_1 - \pi/2,\ \psi_2 - \pi/2]$. Also

$$x(\phi) = b_1\cos\delta_1 - \beta\{2[E(\phi,k) - E(\phi_1,k)] - [F(\phi,k) - F(\phi_1,k)]\},$$

the symbols $F(\phi,k)$ and $E(\phi,k)$ represent the standard Legendre incomplete elliptic integrals of the first and second kinds, correspondingly. From the B.C. of the fullerene at $(b_2\cos\delta_2, C + b_2\sin\delta_2)$ we obtain

$$b_1 \cos\delta_1 - b_2 \cos\delta_2 = \beta\{2[E(\phi_2,k) - E(\phi_1,k)] - [F(\phi_2,k) - F(\phi_1,k)]\}. \tag{4}$$

Given the equation that constrains the length of the arc, we may conclude that

$$c = \int_{b_2\cos\delta_2}^{b_1\cos\delta_1} (1 + y'^2)^{1/2} dx,$$

applying $y' = \tan\theta$ to obtain the following:

$$c = \beta[F(\phi_2,k), F(\phi_1,k)]. \tag{5}$$

Substituting (5) into (4) yields

$$\mu = 2\left(\frac{E(\phi_2,k) - E(\phi_1,k)}{F(\phi_2,k) - F(\phi_1,k)}\right) - 1, \tag{6}$$

with $\mu = (b_1 \cos\delta_1 - b_2 \cos\delta_2)/c$. Consequently, b_1, b_2, δ_1, δ_2 and c are prescribed values. By solving (6) numerically to find k and inserting the obtained result into equation (5), we may determine the value of β, C can be obtained from (3), as demonstrated in Fig. 3.

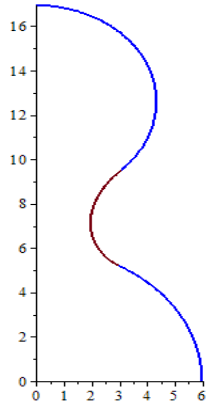

Figure 3: Conjoining profile between fullerene and nanotorus using elastic energy.

3.2. Results via the alternative approach

In this instance, our sought to merge the previous carbon-based structures utilizing the alternative approach as depicted in Fig. 4.

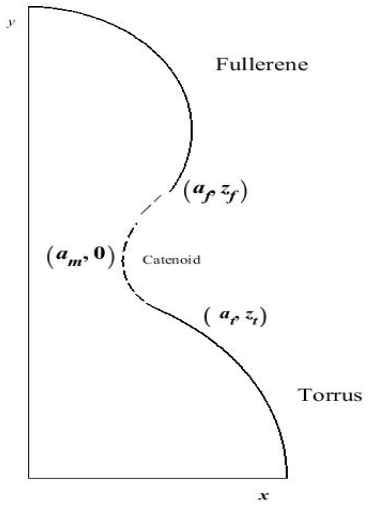

Figure 4: Conjunction geometry of the alternative approach.

The catenoid curve equation can be expressed from (2) as

$$z = \pm \frac{\cosh^{-1}(c_1 a)}{c_1} + c_2, \tag{7}$$

with constants c_1 and c_2 where the positive and negative signs represent the top and bottom catenoid segments, respectively. Here, the top segment joins to a fullerene, whereas the bottom segments joins to a torus. At point $(a_m, 0)$, the differential is equal to ∞ which results $\frac{1}{\sqrt{c_1^2 a_m^2 - 1}} = \infty,$ and,

$$c_1 = \frac{1}{a_m}, \quad c_2 = 0. \tag{8}$$

Now, proceeding under the assumption that the fullerene equation is:

$$z = A_1 - \sqrt{R_1^2 - a^2}, \tag{9}$$

where the fullerene's radius is symbolized by R_1 and A_1 is a constant that pinpointing the centre of the fullerene along the positive z-axis. Subsequently, at $(a_f, z_f),$ (7) and (9), we deduce

$$A_1 = a_m \cosh^{-1}(a_f / a_m) + \sqrt{R_1^2 - a_f^2}. \tag{10}$$

Next, upon aligning the gradients at point (a_f, z_f) we derived $a_f = \sqrt{R_1 a_m}$. Consequently, we find A_1 is the

$$A_1 = a_m \cosh^{-1}\left(\sqrt{\frac{R_1}{a_m}}\right) + \sqrt{R_1(R_1 - a_m)}, \tag{11}$$

By substituting (8) and (11) into (7) and (9) with predefined values of a_m and R_1, thereby establishing the connection to the fullerene.

On the other side, the catenoid merges a torus with torus's equation in Cartesian coordinates as $\left(\sqrt{x^2 + y^2} - R\right)^2 + z^2 = a_1^2,$ and through conversion, we arrive at $x = (R + a_1 \cos\phi)\cos\theta,$ $y = (R + a_1 \cos\phi)\sin\theta,$ $z = a_1 \sin\phi,$ in which θ and ϕ stand for the polar and azimuthal angles in the x-axis and xy-plane, respectively. R represents the torus's major radius whereas a_1 denotes its minor radius. Thus, the equation for the torus in cylindrical coordinates is $(a - R)^2 + z^2 = a_1^2,$ which can be written as

$$z = D + \sqrt{a_1^2 - (a - R)^2}, \tag{12}$$

where D is a constant defined by the torus's place along the negative z-axis [26]. Next, at the intersection point (a_t, z_t), if we consider the negative value of equation (7), which depicts the bottom section of the catenoid, together with equations (8) and (12), we obtain

$$-\frac{\cosh^{-1}(c_1 a_t)}{c_1} = D + \sqrt{a_1^2 - (a_t - R)^2},$$

$$D = -a_m \cosh^{-1}\left(\frac{a_t}{a_m}\right) - \sqrt{a_1^2 - (a_t - R)^2}.$$

Following the gradient alignment, we have $-\frac{1}{\sqrt{c_1^2 a_t^2 - 1}} = \frac{a_t - R}{\sqrt{a_1^2 - (a_t - R)^2}},$

the substitution of (8) allows us to identify $a_t = \frac{\sqrt{4a_1 a_m + R} + R}{2},$ consequently resulting in

$$D = -a_m \cosh^{-1} \frac{\sqrt{4a_1 a_m + R} + R}{2a_m} - \sqrt{a_1^2 - \left(\frac{\sqrt{4a_1 a_m + R} - R}{2} \right)^2}. \tag{13}$$

By substituting (8), (11) and (13) into (7), (9) and (12), respectively, with the given values for a_m, R_1, a_1 and R, we delineate the merging curve between structures via the catenoid curve, as illustrated in Fig. 5.

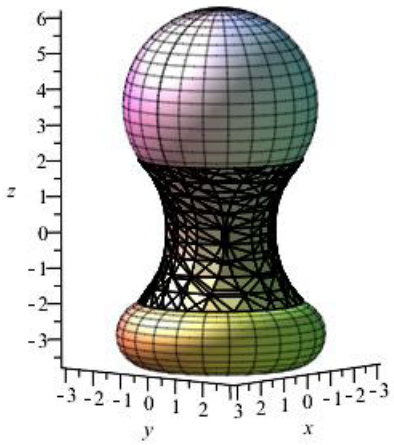

Figure 5: Conjoining profile of fullerene and nanotorus using a catenoid.

4. Conclusions

In this research, the connecting area that connects a fullerene and a nanotorus was pinpointed by evaluating two approaches. In particular, that were produced through the minimization of two separate functionals which depend on the Willmore energy and variational calculus approaches. The integrated structures are foreseen to serve as probes for scanning tunnelling microscopes. The variational calculus approach, which is predicated on minimising the elastic energy of the bending curve, was used to facilitated the determination of this connecting area. The connection among the fullerene and nanotorus was expected to occur at the specified arc length. In the present case, a connecting curve of the nanostructures was established upon scrutinizing the problem in a 2–dimensional space on the xy-plane. The strategy includes utilising the top segment of the catenoid for the fullerene connection while the bottom segment used for nanotorus connection, considering advantage of the catenoid being an optimal minimiser according to the Willmore approach. As a result, these connecting formations are envisioned in a three-dimensional space within the presumption of both structures retain their geometrically flawless shapes without any deformation about their original configurations. Despite the lack of experimental or computational data, these theoretical models seem to provide plausible approximations of these intricate structures and could prove beneficial for future investigations in similar subject. One promising avenue for future work is a model with a nonlocal term which may enhance the model's ability to account for global structural differences between fullerenes and nanotorus, which are not fully captured by local curvature-based models.

References

[1] R.P. Agarwal, B. Xu, W. Zhang, Stability of functional equations in single variable, *J. Math. Anal. Appl.* **288** (2003) 852–869.
[2] J.A. Baker, The stability of certain functional equations, *Proc. Amer. Math. Soc.* **112** (1991) 729–732.
[3] D. Baowan, B Cox, J. Hill. Discrete and Continuous Approximations for Nanobuds, *Fullerenes Nanotubes and Carbon Nanostructures*. **18** (2010) 160–177.

[4] F. D'Souza. Fullerenes, Nanotubes, and Carbon Nanostructures: Carbon Buckyballs to Nanotubes, *Electrochemical Society Interface*. **15** (2006).

[5] O. Shenderova, V. Zhirnov, DW. Brenner. Carbon nanostructures, *Critical Reviews In Solid State And Materials Sciences*. **27** (2002) 227–356.

[6] K. Scida, P. Stege, G. Haby, G, Messina, C. Garcia. Recent applications of carbon-based nanomaterials in analytical chemistry, Critical review. *Analytica Chimica Acta*. **691** (2011) 6–17.

[7] Willmore, T. J. Riemannian Geometry. Clarendon Press, 1993.

[8] P. Sripaturad, N. Alshammari, N. Thamwattana, J. McCoy, D. Baowan. Willmore energy for joining of carbon nanostructures, *Philosophical Magazine*. **98** (2018) 1511–1524.

[9] S. Rouhi, R. Ansari, A. Shahnazari. Vibrational characteristics of single layered boron nitride nanosheet single walled boron nitride nanotube junctions using finite element modeling, *Materials Research Express*. **3** (2016) 1–20.

[10] H. Kroto, J. Heath, S. Obrien et al. C60: Buckminsterfullerene, *Nature*. **318** (1985) 162–163.

[11] D. Dass. Structural and electronic properties of a fullerene with 20, 60, 80, 180, and 240, *Journal of Molecular Modeling*. **26** (2020).

[12] S. Kobayashi, T. Takenobu, S. Mori, A. Fujiwara, Y. Iwasa. Fabrication and characterization of thin-film transistors with high field-effect mobility, *Applied Physics Letters* **82** (2003) 4581–4583.

[13] R. Vasconcelos, V. Aleixo, N. Del. Organic field effect transistor composed by fullerene and heterojunctions, *Physica e-low-dimensional systems and nanostructures*. **86** (2017) 142–145.

[14] A. Mohajeri, A. Omidvar. Fullerene-based materials for solar cell applications: design of novel acceptors for efficient polymer solar cells-a DFT study, *Physical Chemistry Chemical Physics*. **17** (2015) 22367–22376.

[15] S. Pilehvar, K. De Wael. Recent Advances in Electrochemical Biosensors Based on Fullerene Nano-Structured Platforms, *Biosensors-Basel*. **5** (2015) 712–735.

[16] F. Beuerle, C. Herrmann, A. Whalley, C. Valente et al. Optical and Vibrational Properties of Toroidal Carbon Nanotubes, *Chemistry A European Journal*. **17** (2011) 3868–3875.

[17] P. Sarapat, J. Hill, D. Baowan. A Review of Geometry, Construction and Modelling for Carbon Nanotori, *Applied Sciences-Basel*. **9** (2019) 1–20.

[18] C. Feng, K. Liew. A molecular mechanics analysis of the buckling behavior of carbon nanorings under tension, *Carbon*. **47** (2009) 3508–3514.

[19] L. Liu, C. Jayanthi, S. Wu. Structural and electronic properties of a carbon nanotorus: Effects of delocalized and localized deformations, *Physical Review B*. **64** (2001) 033412.

[20] Ansari S, Hassani R et al. Structural stability and buckling analysis of a series of carbon nanotorus using molecular dynamics simulations, *J Mol Mode*. **24** (2018) 263.

[21] D. Baowan, B. Cox, J. Hill J. Determination of Join Regions Between Carbon Nanostructures using Variational Calculus, *Anziam Journal*. **54** (2013) 221–247.

[22] N. Alshammari. Mathematical energy minimization model for joining boron nitride fullerene with several BN nanostructures, *Journal of Molecular Modeling*. **27** (2021) 245.

[23] N. Alshammari, N. Thamwattana, J. McCoy, B. Duangkamon et. al. Modelling joining of various carbon nanostructures using calculus of variations. Dynamics of Continuous, Discrete and Impulsive Systems Series B, *Applications and Algorithms*. **25** (2018) 307–339.

[24] N. Alshammari. Joining between boron nitride nanocones and nanotubes, *Advances in Mathematical Physics*. **2020** (2020) 1–6.

[25] N. Alshammari. Mathematical Modelling for Joining Boron Nitride Graphene with Other BN Nanostructures, *Advances in Mathematical Physics*. **2020** (2020) 1–7.

[26] P. Sripaturad, D. Baowan. Joining curves between nanotorus and nanotube: mathematical approaches based on energy minimization, *Z. Angew. Math. Phys*. **72** (2021) 20.

[27] L. Velimirovic, M. Ciric, M. Cvetkovic. Change of the willmore energy under infinitesimal bending of membranes, *Comput. Math. Appl.*. **59** (2010) 3679–3686.

[28] P. Lim, U. Bagci, L. Bai. Introducing willmore flow into level set segmentation of spinal vertebrae, *IEEE T. BioMed. Eng.*. **60** (2013) 115–22.

[29] C. Bui, V. Lleras, O. Pantz. Dynamics of red blood cells in two D, *EDP Sci*. **28** (2009) 182–194.

[30] C. Szakacs, P. Mezey. Helices of boron-nitrogen hexagons and decagons. A theoretical study, *Journal of Physical Chemistry A*. **112** (2008) 6783–6787.

[31] C. Szakacs, P. Mezey. Theoretical study on the structure and stability of some unusual boron-nitrogen helices, *Journal of Physical Chemistry*. **112** (2008) 2477–2481.

[32] P. Mezey. Energy relations between small and large unit cell boron-nitrogen polymer analogues of spiral graphite and nanoneedle structures, *Journal of Mathematical Chemistry*. **45** (2009) 550–556.

[33] C. Szakacs, P. Mezey. Laterally Extended Spiral Graphite Analogue Boron-Nitrogen Helices, *Journal of Physical Chemistry*. **113** (2009) 5157–5159.

[34] E. Simon, P. Mezey. Imperfect periodicity and systematic changes of some structural features along linear polymers: the case of rod like boron nitrogen nanostructures, *Theoretical Chemistry Accounts*. **131** (2012) 1097.

[35] D. Baowan, B. Cox, J. Hill. A continuous model for the joining of two fullerenes, *Philosophical Magazine*. **88** (2008) 2953–2964.